JOURNAL OF MATERIALS SCIENCE 26 (1991) 5823–5837

Abrasive wear in filled elastomers

A. C.-M. YANG, J. E. AYALA, J. CAMPBELL SCOTT
IBM Research Division, Almaden Research Center, 650 Harry Road, San Jose, CA 95120–6099, USA

The abrasive wear of rubbers is strongly affected by the filler particles dispersed in the elastomer matrix. The fillers are incorporated usually for the purposes of mechanical reinforcement and improving the conductivity of the neat resins. It is found that the wear rates of the filled silicone rubbers increase slowly with filler concentration until a critical volume fraction, v_c, is reached, at which point they increase very rapidly with increasing filler concentration. This behaviour appeared to be universal in all the filled silicones we studied, regardless of the type of filler and silicone rubber used. However the magnitude of the critical filler fraction, v_c, can be changed significantly with the filler shape, resin cross-linking density and filler surface treatments. No reasonable relationship could be found between this wear behaviour and the mechanical properties measured in a macroscopic manner. Experimental evidence suggests that the incipient 'cracks' that lead to wear losses may start within the thin layers of highly stressed material, the 'damage zones', surrounding the rigid particles. A simple model taking into account the stress concentration induced by the rigid fillers shows excellent correlation between the wear rate and the damage zones volume. With this new model, the observed wear behaviours can be explained satisfactorily.

1. Introduction

Engineering rubbers are used extensively in modern technology. In particular, silicone rubbers, noted for their superior thermal stability, are widely employed when elevated temperatures are present during applications. Because they are compliant and tough, the rubbers can easily absorb and survive a single strike of large deformation. However when used in contact with moving parts, a process of micro-tearing can occur on the rubber surface around the sharp asperities, gradually removing the material and finally terminating the functional life of the rubber. In many applications, abrasive wear is the major failure mode of rubbers. Extensive work has been undertaken [1–14] in an attempt to unlock the mysteries behind the wear phenomena, yet the underlying mechanisms are not fully understood and few predictive models of wear can be found in the literature. This is due to the extremely complex nature of wear in rubbers. For example, many testing parameters will not only change the measured wear rate quantitatively, but will also qualitatively alter the governing mechanism of the wear process.

Nevertheless, since abrasion is clearly a manifestation of mechanical failure, people have been trying to relate it to material fracture. Shallamach [1, 9] used tearing energy to describe the rubber wear mechanisms, and Ratner [4–6] has established an equation in which the wear loss is related to macroscopic mechanical properties such as tensile strength, elongation at break, hardness etc. But since the local fractures that eventually lead to abrasive wear are several orders of magnitude smaller in scale than these in which the macroscopic properties are determined, it is curious to learn whether Ratner's equation can be applied to systems that are heterogeneous in nature, e.g. filled rubbers. Fillers have long been used to impart or improve the properties in various materials, and are indeed a major component of modern engineering rubbers where the filler fraction can be as high as 70 wt % of the material. The role of filler in abrasive wear needs careful study.

In this paper we consider how filler particles influence rubber wear. The wear rates are measured as functions of filler concentration, filler type and filler shape, as well as filler surface treatments and the resin cross-linking density. Ratner's equation is examined with the macroscopic mechanical data. Finally, a new micro-mechanical model is presented to explain the observed phenomenon.

2. Experimental procedure

The sample of a filled rubber was prepared by first thoroughly blending a filler with poly(dimethyl siloxane) (PDMS) rubber at room temperature, and then cured at 170 °C for 30 min in a mould. The cured sample was then removed from the mould and post cured in an oven for 1.5 h at the same cure temperature. Before any curing occurred, the fluid mixture was degassed in a vacuum chamber to remove air bubbles that were introduced during mixing. Two types of PDMS were used: a commercial resin, Dow Corning Sylgard S-182, and vinyl-terminated PDMSs

0022–2461/91 $03.00 + .12

from Petrarch Systems, with different molecular weights of 6,000, 17,250 and 120,000. The vinyl terminated PDMSs were cross-linked using a methylhydro dimethylsiloxane copolymer with chloro-platinic acid inhibited with propargyl alcohol that became active above 80 °C. The Sylgard 182 rubber was crosslinked with the cure agent from Dow Corning. The filler was selected from one of the following fine powders of zinc oxide, alpha-iron oxide, aluminium oxide, mica flakes, small glass beads and short glass fibres. Some of the small glass beads and mica flakes were surface treated with organic coupling agents before arrival.

According to the particle geometry, the fillers can be grouped into three categories: (i) spherical particles: zinc oxide, α-iron oxide, aluminium oxide and small glass beads; (ii) platelets: micas; and (iii) short fibres: the short glass fibres. The particle size and aspect ratio of one filler vary over a broad range, but the mean values are obtainable by averaging measurements on images, usually around 30, from the SEM micrographs. For the spherical particles, the zinc oxide and the iron oxide particles are very small with an average diameter approximately equal to 0.1 μm for zinc oxide, and 0.2 μm for iron oxide. The aluminium oxide appears to have an even wider distribution with an average diameter of approximately 10 μm, considerably larger than those of the zinc oxide and iron oxide particles. Comparable in size to the aluminium oxide particles are the small glass beads which have a diameter range from 1 to 40 μm. The average dimensions of the platelet mica are roughly 30 by 0.2 μm, and the glass fibres 50 by 10 μm.

The cured sample has a thickness of approximately 2 mm and is cut into a disc of 10 cm in diameter for wear testing. The disc sample is mounted on a rotating stage in a Taber Abraser that rotates at a fixed angular speed, ~ 60 r.p.m. A pair of abrading wheels, the standard H-18 calibrase wheels, contact from the top of the sample surface with a weight of 500 g and a counter weight of 125 g on the other end of the abrading arm. A pair of suction nozzles were positioned slightly above the sample surface to remove the worn debris during the wear test. The abrading wheels were refaced while the weight loss in the filled rubber was measured every 1000 revolutions. The worn surface was gently cleaned by air gun before the weight measurement was taken. SEM was used to study the worn rubber surfaces.

The mechanical properties, tensile strength, elongation at break and Young's modulus, of the rubber composites were measured by using an Instron 1122 in a standard uniaxial tensile test. The tearing energy was obtained in a similar way by measuring the force required for propagating a crack in a trouser-type specimen at a constant speed (25.4 mm s^{-1}). The specimen surfaces were taped so that the crack would propagate straight along the centre of the specimen, allowing consistent and reliable measurements to be taken. The taping may cause the measured force to be slightly higher than that of an untaped specimen, but this effect seems to be independent of the specimens so the data obtained appears to be a reliable measure of the tearing energy. The friction coefficients were measured by using a friction and slip tester from Testing Machines Inc. A sand paper of grit 220 was used as the counter face in the test because the asperity spacing, as revealed by using an optical microscope, is close to that of the standard H-18 calibrase wheels (around 100 μm). The hardness of the filled rubbers were measured by a Shore A Durometer.

The adhesion strength at the filler/rubber interface was estimated by measuring the peel force of a thin layer of PDMS cured on an oxide-deposited substrate. A thin layer (110 nm thick) of the filler substance, e.g. ZnO, was deposited by reactive RF sputtering on a glass slide and then a layer of silicone rubber was cured on top of the coating. Peel force was measured as a function of the PDMS layer thickness and the adhesion strength was obtained from the extrapolation of the peel force at either zero or infinite thickness where the plastic deformation becomes negligible during peeling (Brown and Yang, *J. Adhesion Sci. Technol.*, in press). The peel rate was held constant at 25.4 mm min^{-1}.

3. Results and analysis

The wear properties of composites with different filler particles were compared by measuring the wear rates in a Taber abrader. The wear rate of each composite was obtained from the slope in a plot of the total wear weight loss against the number of abrasion revolutions. The initial data point of the first 1000 revolutions that involved the removal of the top surface was discarded to eliminate the effect of possible contamination and damage to the sample external surface. A linear relationship was generally followed by the data points, indicating that the wear rate was well defined. Since the abraded surface had been roughened after 1000 revolutions, the wear rates so obtained represent those of steady-state wear.

Fig. 1 shows the plot of the wear rates of the composites against filler weight fraction for the various fillers. In all the curves, a common trend of the wear rate with the filler fraction can be clearly observed: as the filler fraction increases, the wear rate increases slowly until the filler fraction reaches a break point, called the 'critical filler fraction', after which the wear rate starts to increase very quickly with increasing filler fraction. The critical filler fraction should carry important information, as it apparently divides two wear regimes dominated by different mechanisms. The first regime where the filler fraction is low seems to be dominated by the intrinsic wear process of the neat resin. The second regime, on the other hand, appears to be controlled by the weakening effect of the filler particles. The weakening effect of the filler particles, however, looks remarkably similar for all three classes of fillers. The wear rates of all the materials rise sharply in the second wear regime, approaching a straight line. The only exceptions are the materials filled with mica particles, where the rapid increase in wear rate tends to slow down eventually and the wear rate levels off. Nevertheless, the critical filler fraction, which represents the onset of the second regime, is a

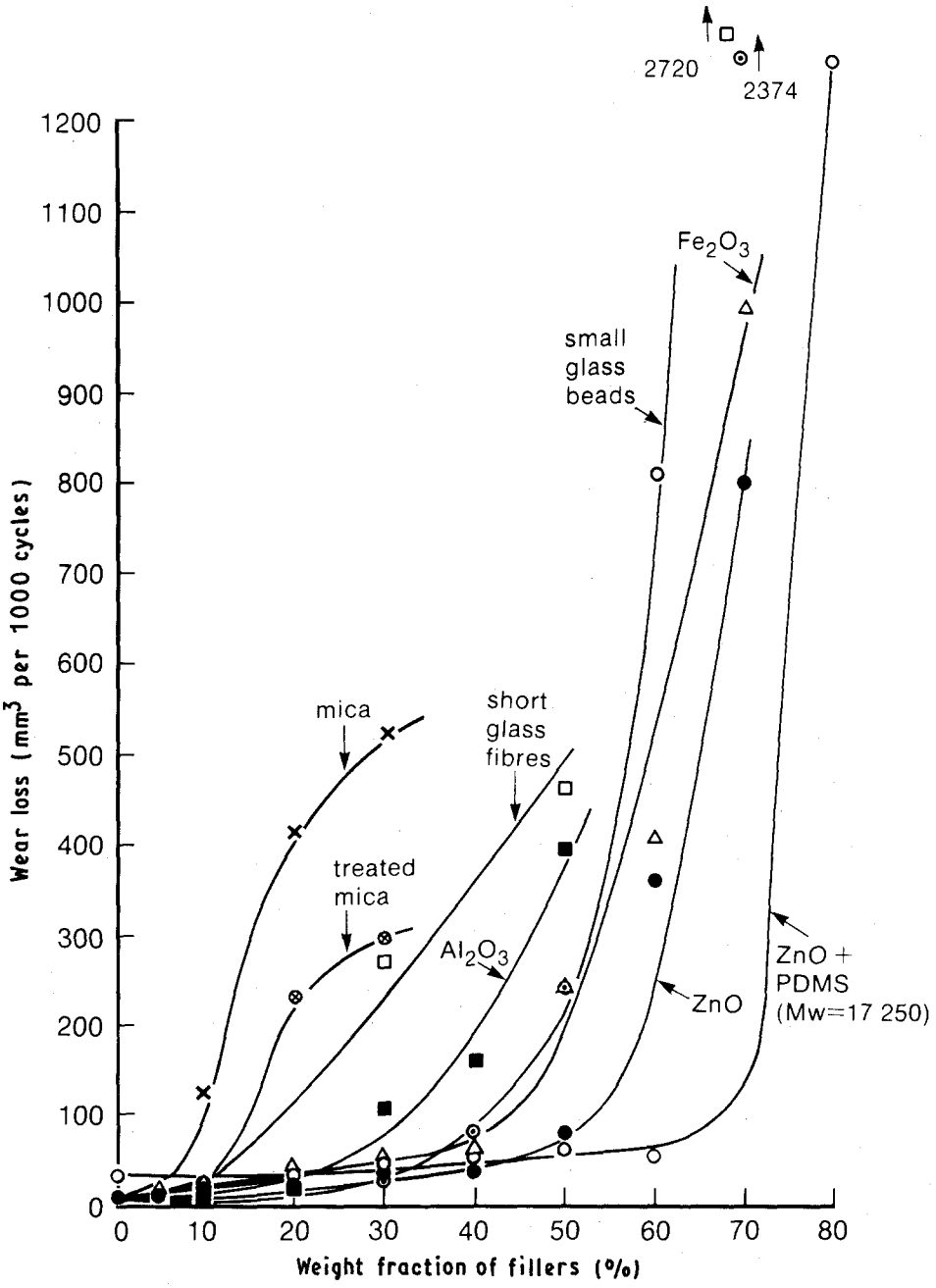

Figure 1 Wear rates against filler weight fraction (filler in S-182).

sensitive function of the particle geometry and, for larger filler particles, particle surface treatments. Consistent with previous results (A. C.-M. Yang *et al.*, *Wear*, in press), the critical filler fractions for short glass fibres and micas are significantly lower than those of the spherical particles. Also, in the case of micas, the critical filler fraction increases when the filler–matrix interaction is enhanced by the organic surface treatment.

The wear data of Fig. 1 are plotted again in Fig. 2 in terms of wear volume and filler volume fraction. The shape of each curve remains unchanged, maintaining a clear break point at the critical volume fraction. Due to the difference in particle density, the curves shift horizontally, yet the conclusions drawn previously remain valid, i.e. the platelets and short fibres have lower critical filler fractions. However, it is noteworthy that the curves of the zinc oxide, iron oxide and aluminium oxide particles now converge together in this plot in both the first and the second regimes, as shown in Fig. 2. The only spherical particles that do not converge are the small glass beads which show a higher critical filler fraction. It is thus interesting to examine why the three different fillers follow a single curve, and yet why the glass beads behave differently. The quasi-universal behaviour of the three spherical particles seems to indicate that the spatial arrangement of the filler particles in the rubber matrix plays a crucial role in the wear of composites. On the other hand, the fact that the glass beads follow a different curve indicates that some important parameters other than just the filler occupation in the matrix must also be taken into account.

Before we proceed further in comparing different filler particles, we first focus our attention on one representative species, say zinc oxide, and try to understand the characteristics of the wear rate against filler fraction. The worn surfaces and the wear debris

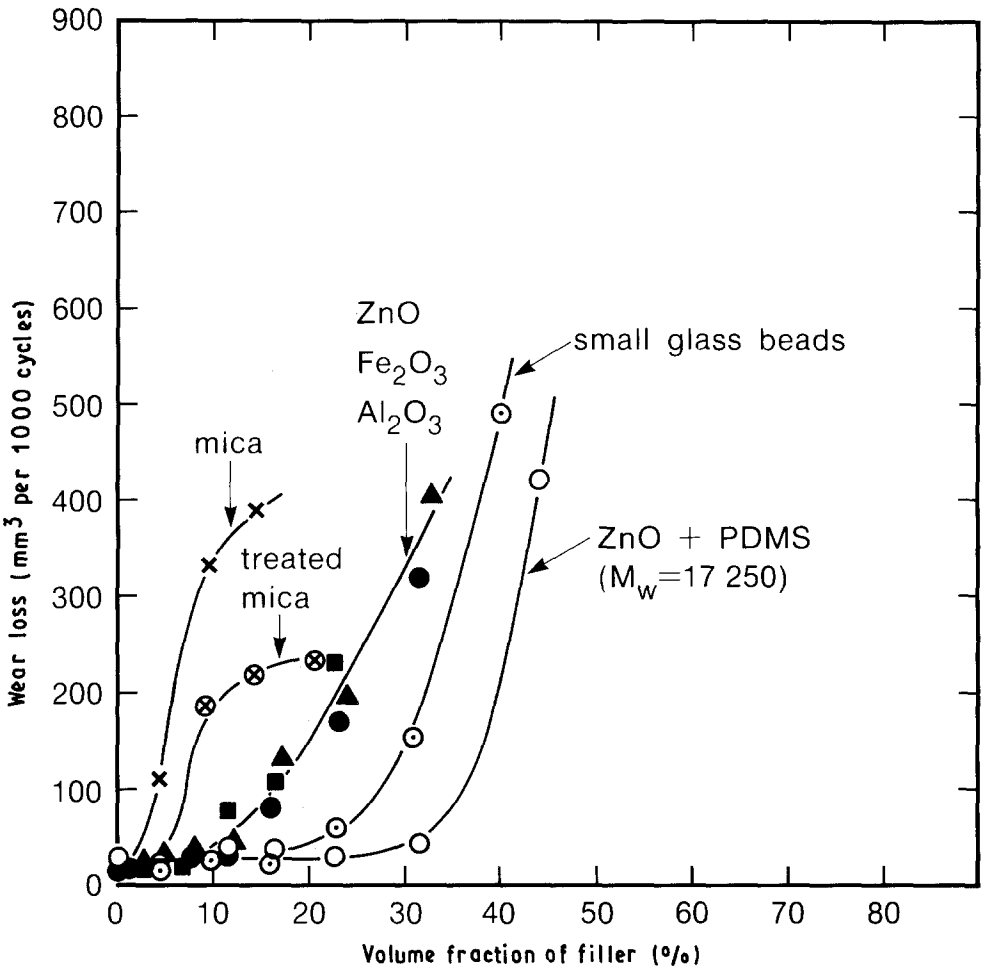

Figure 2 Wear rates against filler volume fraction (filler in S-182). ●, ZnO; ▲, Fe_2O_3; ■, Al_2O_3.

were examined under SEM. We found that the worn surfaces of the composites of lower filler content were much smoother than those of higher filler concentrations. Except the large ploughing lines that cross each other, there are few features on the worn surface, for example of the neat resin as shown in Fig. 3a. Reflecting this topography, the wear debris of the neat resin are large, round and smooth at the external surfaces (Fig. 3b). As the filler concentration increases, the worn particles become more and more coral-like (Fig. 3d); microscopically, the debris are smaller as they contain features in fine scales, but because of the interconnected structure between the wear debris, macroscopically the worn particles of the higher filler concentrations appear to the naked eye to be larger than those of the lower filler concentrations. The worn surfaces of the composites of higher filler concentration show signs of micro-tearing with a wear pattern of ridges and valleys in the lateral scales of 10 μm (Fig. 3c).

Since micro-tearing seems to prevail during the abrasion, the connection between wear rate and macroscopic mechanical properties that are usually cited in existing wear models were examined. According to Ratner *et al.* [4–6] the abrasive wear can be described by the following equation

$$\frac{V}{L} = K\mu \frac{W}{H\sigma_b\varepsilon_b} \quad (1)$$

where V/L is the volume of worn material per unit length of sliding, μ the friction coefficient, W the load at contact, H the indentation hardness, σ_b the tensile strength, ε_b the elongation at break of the polymeric material, and K a proportionality constant. Ratner's equation works well with the unfilled neat resins, where a good correlation of wear rate with the product $\sigma_b\varepsilon_b$ has been found for silicone rubbers (A. C.-M. Yang, unpublished data). To test the model further, for the filler rubbers the hardness of the materials was measured in Durometer Shore A. Fig. 4a shows that the Durometer increases monotonically with the filler fraction for zinc oxide, iron oxide and small glass beads. The tensile strength, σ_b, and the elongation at break, ε_b, measured from Instron, are not as straightforward as is the durometer, as shown in Fig. 4b and c. The two quantities always fall as a small amount of filler is added to Sylgard 182 binder. As the filler concentration increases further, they go through a minimum, increase and finally decrease again. Although each data point fluctuates, the characteristics of the curves between the data points are remarkably reproducible, and are repeated for different filler particles. Friction coefficients, μ, were measured as a function of zinc oxide concentration, and were found to be virtually constant with filler concentration. Since the load W is constant, the quantities $1/(H\sigma_b\varepsilon_b)$ for the three fillers are plotted against the filler fraction in Fig. 3d. If Ratner's model

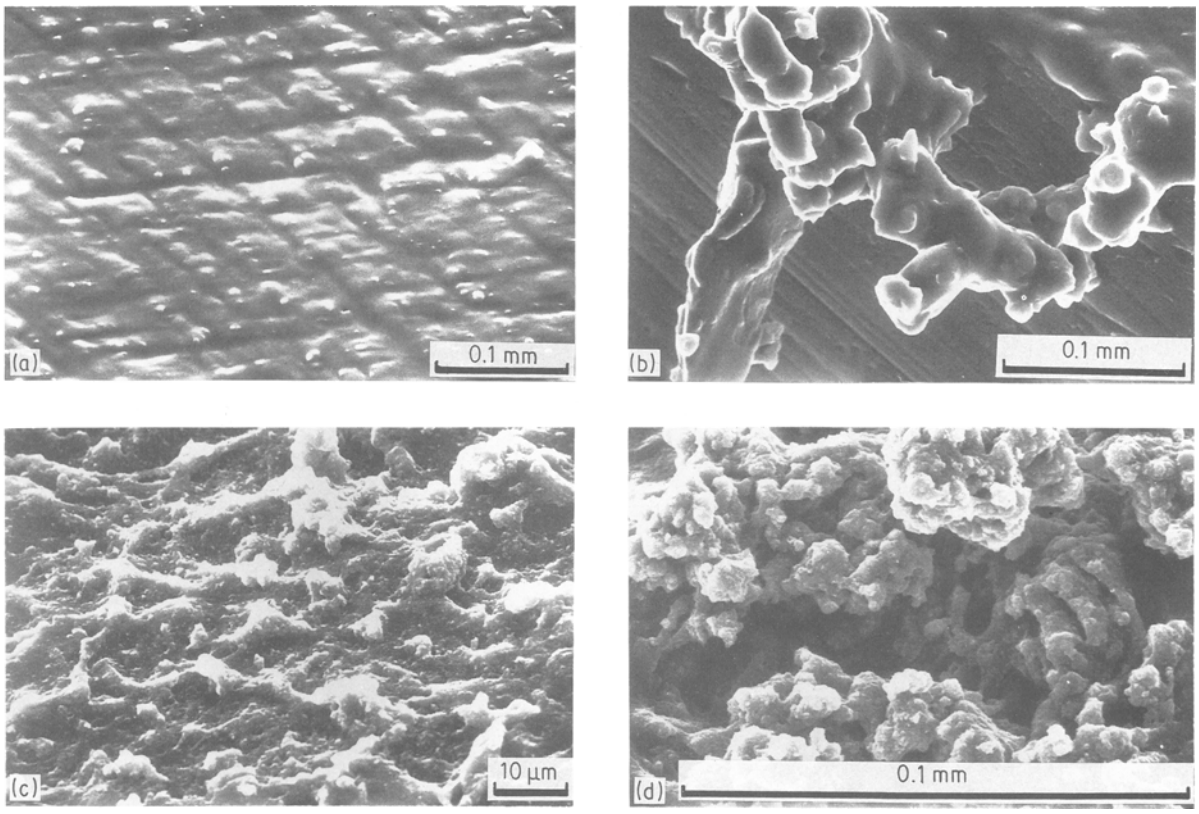

Figure 3 SEM micrograph of (a) worn surface of the neat Sylgard 182 elastomer; (b) worn particles of the neat Sylgard 182 elastomer; (c) worn surface of the elastomer filled with 70 wt % zinc oxide; (d) worn particles of the filled elastomer with 70 wt % zinc oxide.

(Equation 1) is applicable here, we would expect to see curves very similar to those of the wear rate in Figs 1 and 2. But by comparing Figs 1 and 3d, we conclude that no linear relationship exists between the quantity $1/(H\sigma\varepsilon)$ and the wear rate, and hence that Ratner's equation is not applicable in this class of materials.

As a further check, a different silicone binder, a vinyl terminated PDMS ($M_w = 17\,250$), was used with the zinc oxide filler particles and its wear rate and mechanical properties were measured. The results are plotted, along with the data of the Sylgard 182 composites, in Figs 1, 2 and 4. The same characteristics in wear, as seen in the previous materials, were observed again even though the tensile strength was qualitatively different from the previous systems: the tensile strength σ_b monotonically increases with the filler fraction. This confirms that the macroscopic tensile properties have little connection with the abrasive wear in rubber composites, and that approaches other than Ratner's equation should be explored.

The discrepancy between our data and Ratner's equation probably can be understood from the fact that the macroscopic tensile properties were generally determined by the weakest linkage in the materials, i.e. any dominant flaws or stress concentrators. A single crack initiator can cause the whole bulk sample to fail and thus dramatically change the mechanical properties. On the other hand, abrasive wear is a cumulative process of failures of the length scale comparable to that of the counterface asperities. Micro-tearing, as strongly suggested from the topography of the worn filled rubbers shown in Fig. 3, takes place locally, contributing to the total wear loss of the samples. A single stress concentrator can only produce limited effects on the wear test results. Because of their difference in developing the failures, it is conceivable that a straightforward one-to-one correspondence between wear loss and macroscopic tensile properties could not be found.

This same argument probably can also be used to explain the poor correlation between wear and the critical tearing energy release rate G_c, as shown in Fig. 5.

In an attempt to explore approaches other than Ratner's model, the effects of filler in a composite on the mechanical response to an applied external deformation were considered. Because the Young's modulus of the filler particles is so large compared with the soft rubber, the filler can be regarded as rigid. As these rigid particles are added into the soft rubber matrix, an external strain causes deformation only in the rubber phase, resulting in enhanced local strain [15]. The ratio of the effective strain in the rubber to the applied strain on the whole composite, called the strain amplification factor, ξ, increases as the filler concentration increases. It is interesting to note that the strain amplification factor ξ initially increases slowly with decreasing particle spacing before reaching a critical spacing, after which it takes off very quickly, as shown in Fig. 6. This behaviour is remarkably similar to that of the wear rate in the composites. Therefore, the spatial arrangements of the filler particles in the rubber matrix and the stress fields around each filler particle are important when considering the

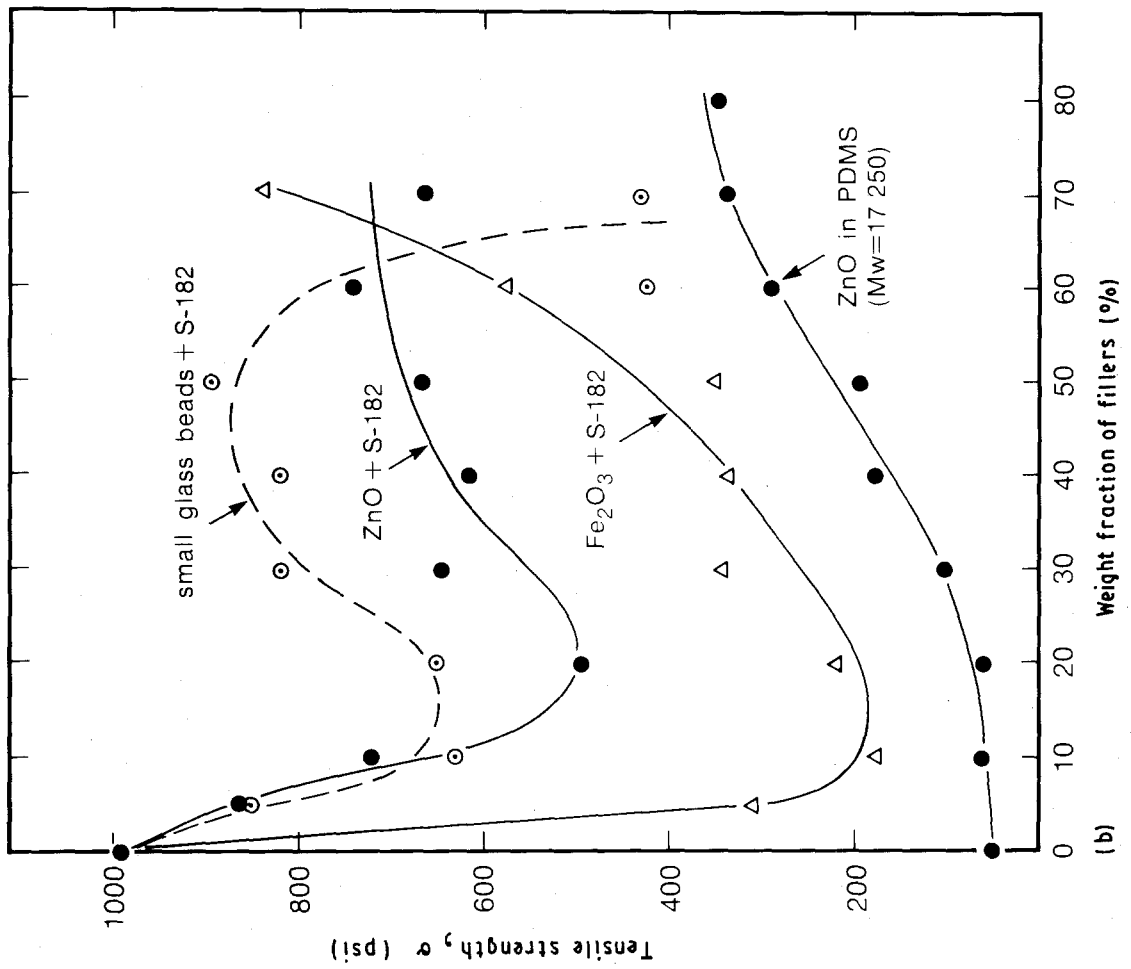
Tensile strength, σ (psi)
1000
800
600
400
200
small glass beads + S-182
ZnO + S-182
Fe_2O_3 + S-182
ZnO in PDMS
(Mw=17 250)
0
10
20
30
40
50
60
70
80
Weight fraction of fillers (%)
(b)

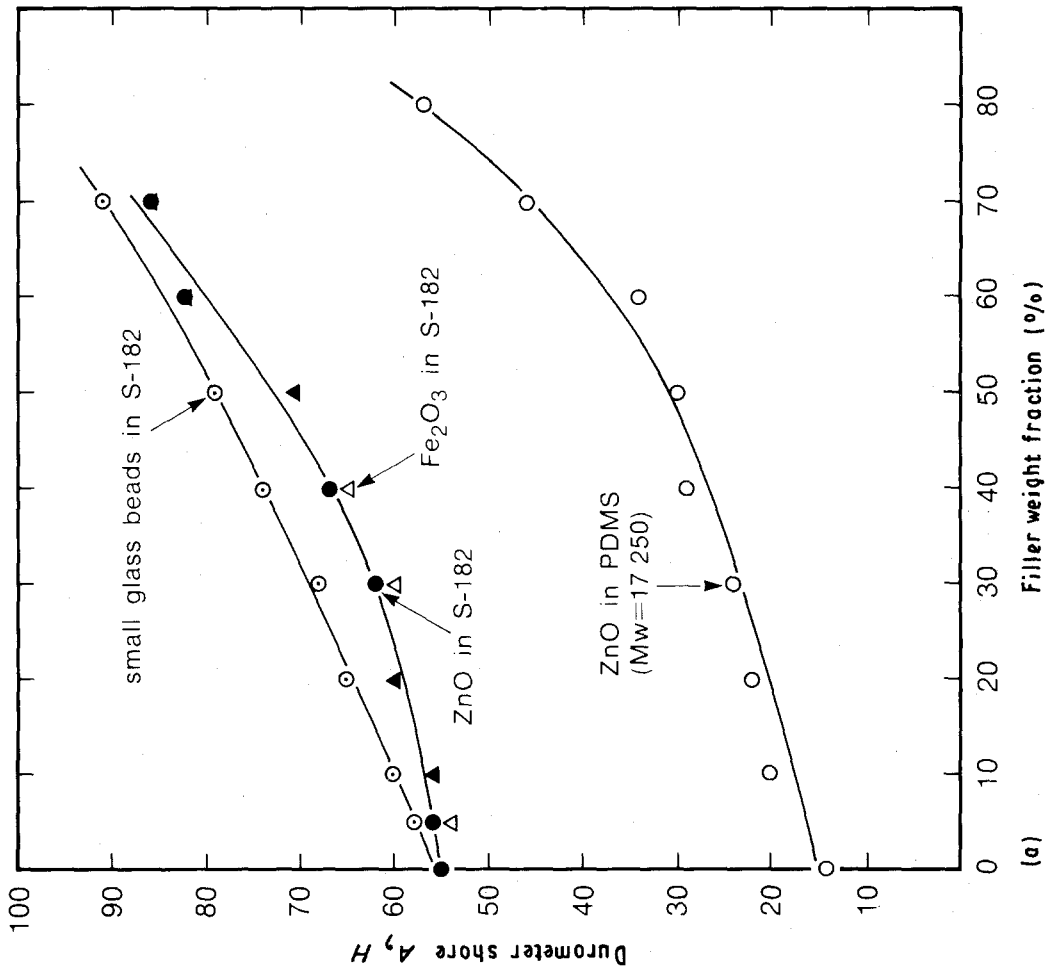
Durometer shore A, H
100
90
80
70
60
50
40
30
20
10
small glass beads in S-182
Fe_2O_3 in S-182
ZnO in S-182
ZnO in PDMS
(Mw=17 250)
0
10
20
30
40
50
60
70
80
Filler weight fraction (%)
(a)

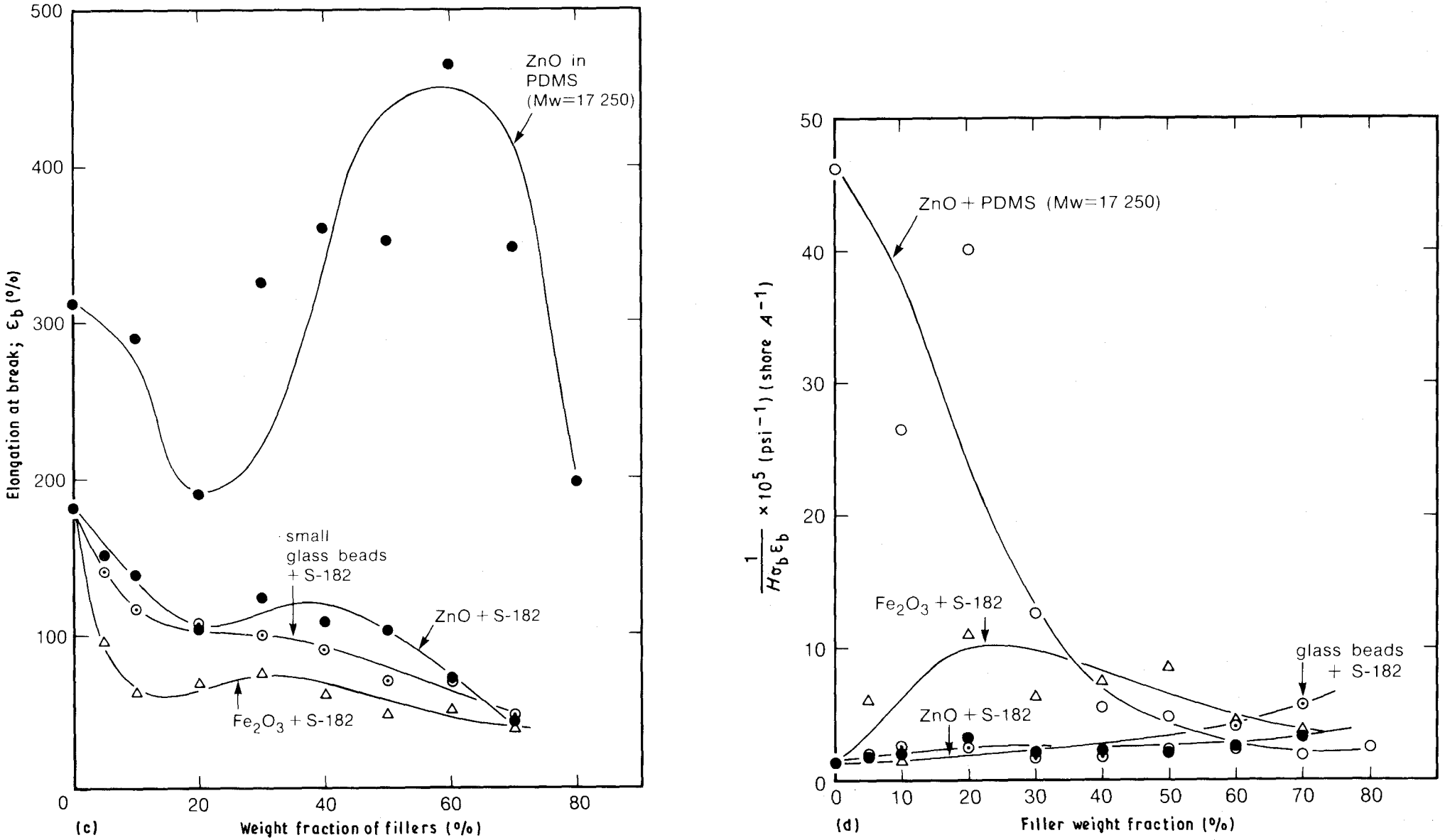

Figure 4 (a) Durometer H; (b) tensile strength σ_b; (c) elongation at break ε_b; (d) $1/(H\sigma_b\varepsilon_b)$ against filler weight fraction.

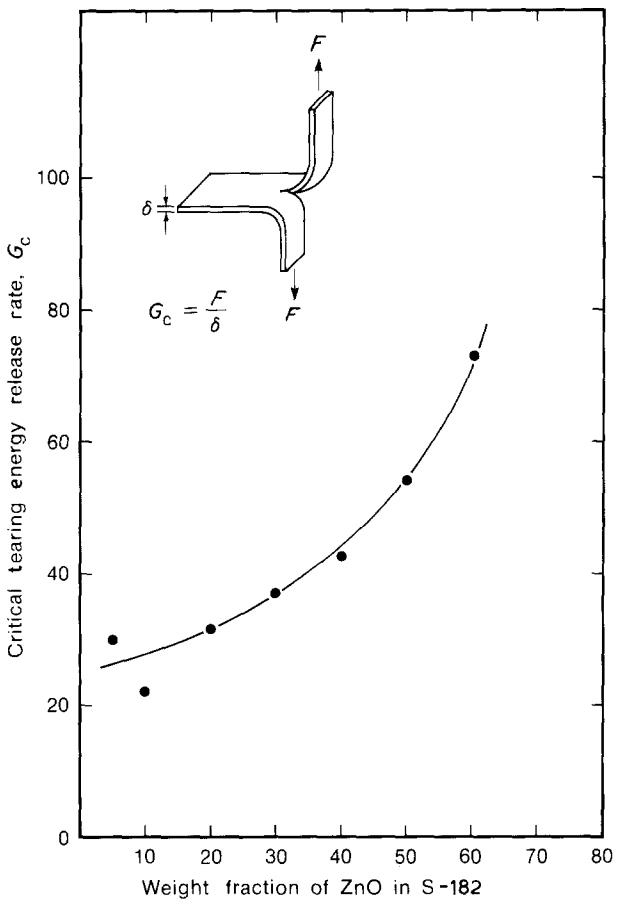

Figure 5 Critical tearing energy release rate, G_c, as a function of zinc oxide concentration.

wear in a rubber composite. The reason that the composites of zinc oxide, iron oxide and aluminium oxide in the Sylgard 182 matrix all follow a single curve of wear against filler fraction is probably due to the fact that they are all spherical particles, and the stress fields associated with the particles are similar.

The local stress field can be examined analytically. At the presence of an applied load, the rigid particles in the soft matrix can act as stress concentrators, inducing a larger and more complicated stress field, than that applied, in their surroundings. The stress field around a spherical particle in a matrix, solved previously by Goodier [11, 16] can be expressed as

$$\frac{\sigma_{\mathbb{R}}}{T_\infty} = \frac{a_0^3}{r^3}(1 + 3\cos 2\theta)\left(\frac{5}{4} - \frac{a_0^2}{r^2}\right) + 1$$

$$\frac{\sigma_{\theta\theta}}{T_\infty} = \frac{a_0^5}{4r^5}(1 + 7\cos 2\theta)$$

$$\frac{\sigma_{\phi\phi}}{T_\infty} = \frac{a_0^5}{4r^5}(3 + 5\cos 2\theta)$$

$$\frac{\sigma_{r\theta}}{T_\infty} = 2\frac{a_0^3}{r^3}\left(\frac{5}{8} - \frac{a_0^2}{r^2}\right)\sin 2\theta \qquad (2)$$

where T_∞ is the externally applied stress in the direction of $\theta = 0$, a_0 the particle radius, r the distance from the centre of the particle, $\sigma_{r\theta}$ the shear stress, and $\sigma_{\mathbb{R}}$, $\sigma_{\theta\theta}$, $\sigma_{\phi\phi}$ the normal stresses in the three principal axes, as shown in Fig. 7. Here we have assumed that Poisson's ratio of the rubber, ν_1, is equal to 0.5 and Young's modulus of the filler particles, E_2, is equal to infinity. At the poles of the rigid spherical inclusions, i.e. at $\theta = 0$ and π, the shear stress $\sigma_{r\theta}$ vanishes and a dilatational tri-axial tension, τ, operates. The three components of the normal stresses in the principal axes can be written from Equation 2 as

$$\frac{\sigma_{\mathbb{R}}}{T_\infty} = 1 + 5\frac{a_0^3}{r^3} - 4\frac{a_0^5}{r^5}$$

$$\frac{\sigma_{\theta\theta}}{T_\infty} = \frac{\sigma_{\phi\phi}}{T_\infty} = 2\frac{a_0^5}{r^5} \qquad (3)$$

The induced components, $\sigma_{\mathbb{R}} - 1$, $\sigma_{\theta\theta}$, $\sigma_{\phi\phi}$, at the poles are plotted against the distance from the particle, r/a_0 in Fig. 7, where the stress $\sigma_{\mathbb{R}}$ shows a maximum around $r/a_0 = 1.2$ while the stresses $\sigma_{\theta\theta}$ and $\sigma_{\phi\phi}$ decrease inversely with the fifth power of the distance. The tri-axial tension, $\tau \equiv |\sigma_{\mathbb{R}} + \sigma_{\theta\theta} + \sigma_{\phi\phi}| = 1 + 5(a_0/r)^3$, consequently decreases inversely with the third power of the distance r. Because of this locally amplified dilatation, conceptually there exists a layer of highly stressed region, a so-called 'stressed zone', surrounding each rigid particle. Within this stressed zone, microscopic damages that eventually lead to catastrophic fracture and wear failures are more likely to take place than in other areas.

Gent and Park [11] have shown that for the case of a single glass bead inclusion in a silicone elastomer, debonding at or cavitation near the bead surface can happen when the composite is under tension. They reported that the two mechanisms have different dependences on the Young's modulus, E_1, of the rubber matrix. The critical cavitation stress σ_k measured was found to increase with the Young's modulus, E_1, following the empirical equation of Hall [17] and Petch [18]

$$\sigma_k = AE_1 + B(d)^{-1/2} \qquad (4)$$

where d is the diameter of the glass bead, and A and B are constants. On the other hand, the critical stress for debonding decreases with Young's modulus, E_1. If either debonding or cavitation, or both, initiate at the stressed zones and contribute to the final wear, we would expect to observe a considerable effect on wear due to the matrix modulus E_1 and the adhesion strength at the rubber/particle interfaces.

It is therefore constructive to measure, or estimate, the adhesion strength at the interface. To serve our purpose, peel tests were conducted on specimens made by curing a uniform layer of silicone rubber on a substrate. The substrates were a layer of thin film ZnO or iron oxide, deposited by sputtering on a glass slide; a bare clean glass slide; and a surface-oxidized aluminium plate. The adhesion strength of the thin film ZnO and Fe_2O_3 to the substrate was strong enough to avoid any difficulty in successfully peeling the silicone layer from the surface of the ZnO or Fe_2O_3. The peel strengths were recorded to estimate adhesion strength at the various filler/rubber interfaces. Since the rubber arm can dissipate a portion of the mechanical energy during peeling action, the peel strength was measured

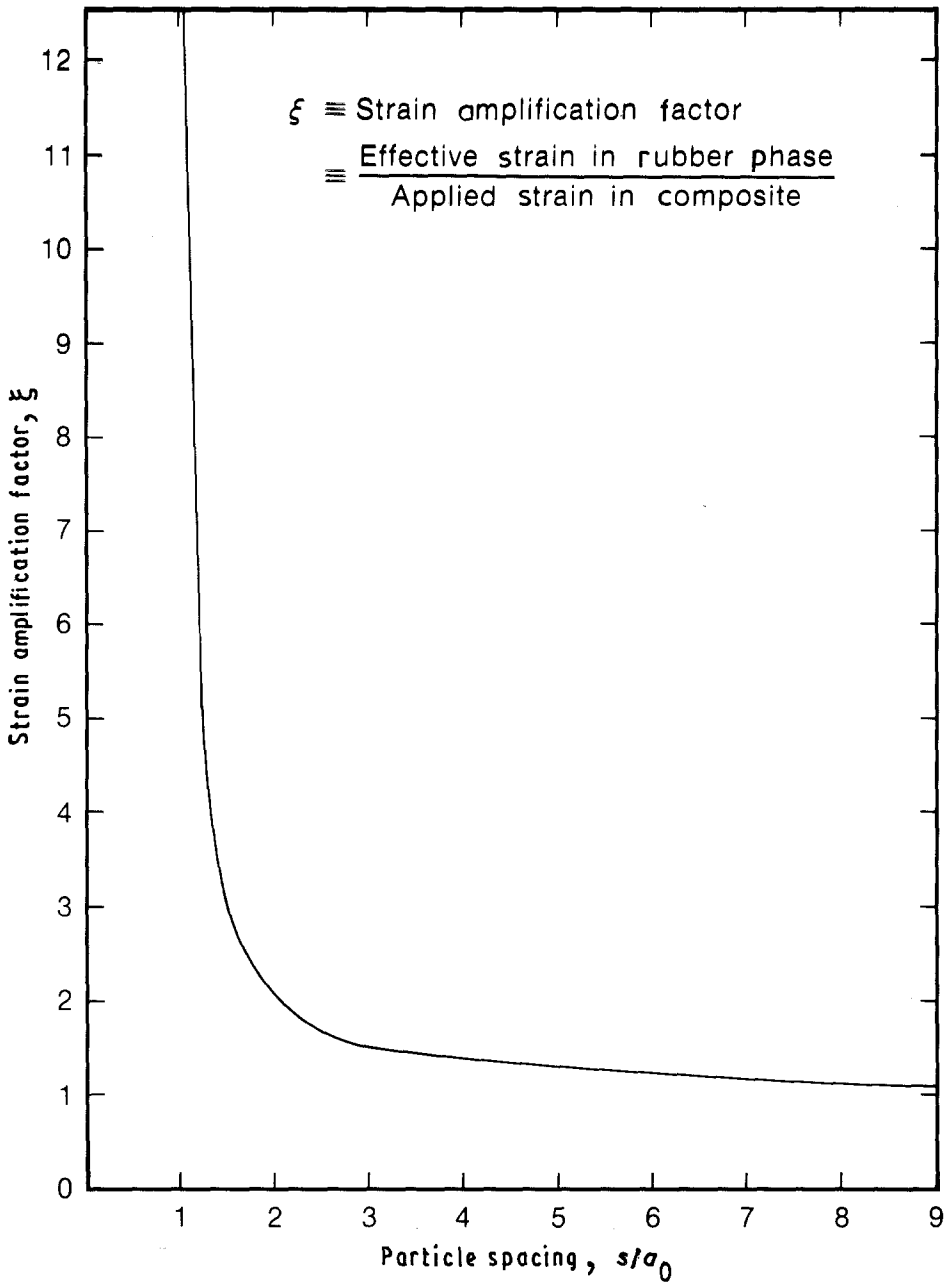

Figure 6 Strain amplification factor ξ as a function of particle spacing in a model of two dimensional approximation.

as a function of rubber thickness, allowing the intrinsic adhesion strength at the interface to be obtained by extrapolation, from the peel strength at both thickness extremes, i.e. 0 and ∞, where the work of deformation becomes negligible (Brown and Yang, *J. Adhesion Sci. Technol.*, in press). The peel test results are plotted in Fig. 8. They show that the bare glass and iron oxide apparently have higher adhesion at the rubber interfaces when compared with those of zinc oxide and aluminium oxide. If these data, obtained in bulk samples, are the true measures of the interfacial strengths between the small particles and the neat resin, it would appear that a correlation between wear and debonding is lacking. If, however, we postulate that the peel test results are only reliable down to a certain particle size, below which debonding becomes increasingly unfavoured, the peel test data are in fact quite consistent with the observed wear behaviours. For example, in the category of larger particles (glass beads and aluminium oxide), lower wear rates were found where the higher peel strengths were measured. Also, as shown in Figs 1 and 2, the wear rate is significantly lower for the surface-treated mica than for the untreated counterparts. A similar effect was also found (A. C.-M. Yang *et al.*, *Wear*, in press) for large glass beads with diameters from ~ 5 to $\sim 1000\,\mu m$. These results strongly suggest that a debonding process is involved during abrasion in the rubbers filled with the large particles. We may postulate that as the particle size decreases, the debonding mechanism becomes unfavoured, and instead the other mechanism of micro-cavitation starts to dominate when the material is under dilatation. Then for tiny filler particles, as in the cases of zinc oxide and iron oxide particles, the adhesion strength at the particle/rubber interfaces will consequently become less important in wear failure development.

To try to support this picture, the cross-linking density and hence the Young's modulus, E_1, of the rubber matrix was changed to examine its effect on

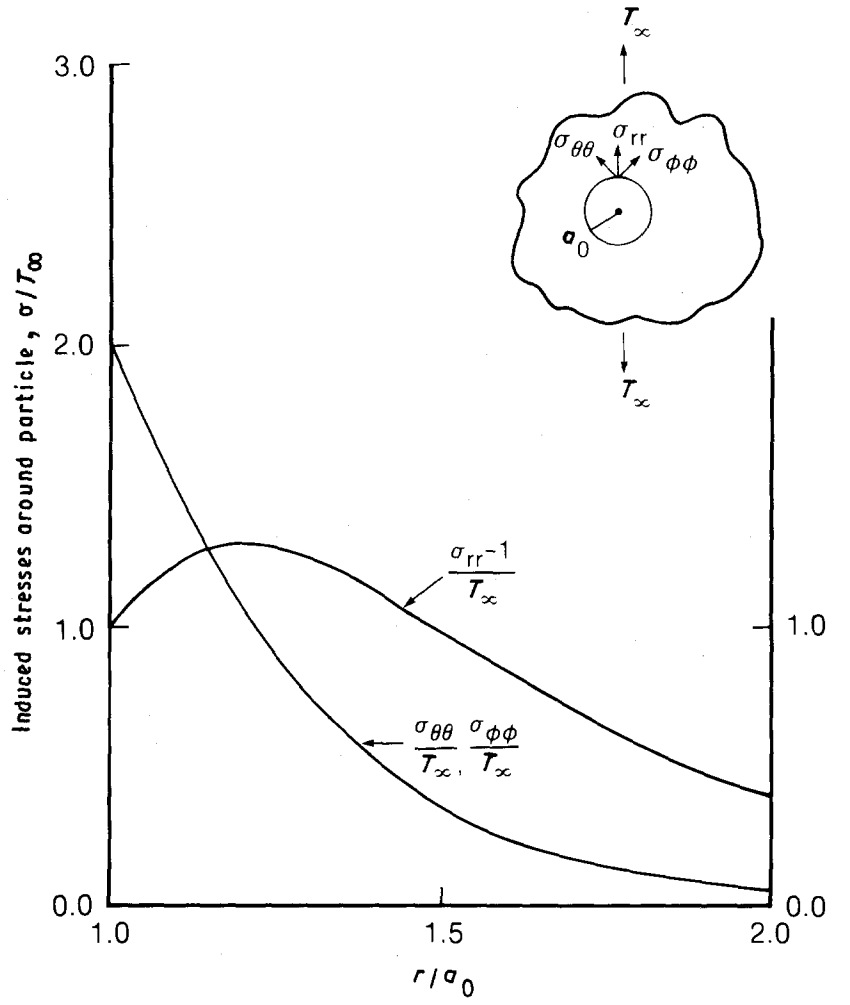

Figure 7 Induced stress distribution around a rigid particle in a soft matrix.

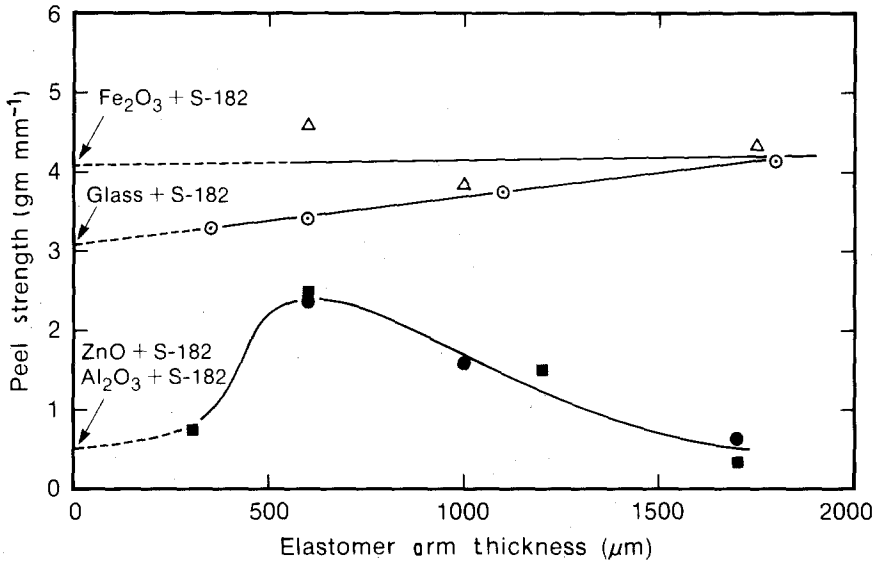

Figure 8 Peel strength of layered samples against arm thickness.

wear. From Equation 4, the critical cavitation stress, σ_k, increases linearly with E_1. Three different molecular weights (6000, 17 250 and 120 000 kDa) of the vinyl-terminated PDMSs were blended with zinc oxide and cured. The wear rate against zinc oxide concentration for the three matrices of different cross-link densities is shown in Fig. 9. The mechanical properties of the neat resins were measured and are presented in Table I. The three neat resins are very weak compared to the commercial grade of Sylgard 182. It was noticed that although the composites of the 6000 kDa matrix generally wear faster than the other two, a fact we believe to be due to the very weak matrix, the critical filler fraction, v_c, for zinc oxide is

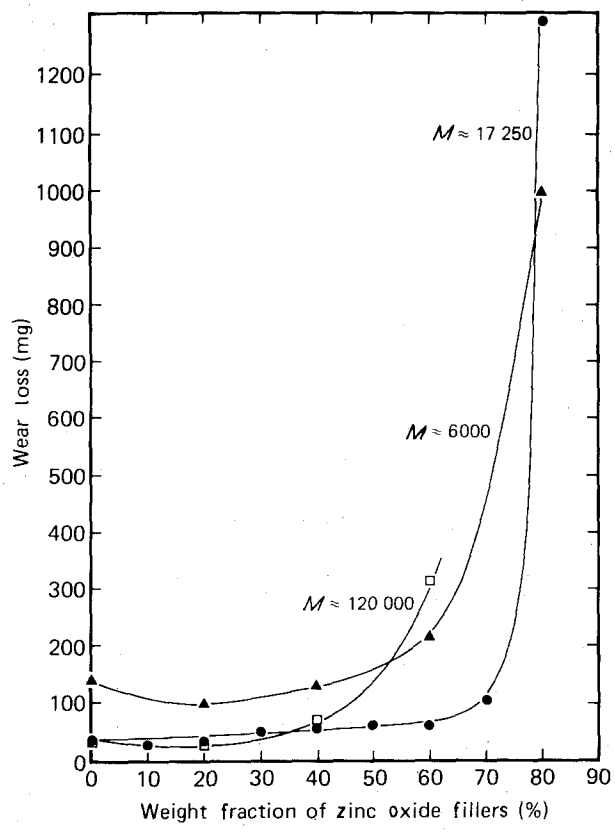

Figure 9 Wear rates against filler concentration for the three molecular-weight matrices filled with zinc oxide (ZnO in PDMS).

significantly larger than those of the highest molecular-weight composites. The comparison becomes more evident in Fig. 10 where the wear rates are normalized to those of the neat resins and plotted against the particle spacing which was calculated from the filler concentration. It shows that the three curves overlap closely in the first wear regime, and the wear rate of the highest molecular weight (120 000 kDa) increases rapidly at the highest critical particle spacing. On the other hand, the Young's modulus E_1 decreases as the molecular weight increases, from 120 p.s.i. for $M_w = 6000$ to 30 p.s.i. for $M_w = 120\,000$ (Table I). Compared with the relation between the Young's modulus E_1 and the cavitation stress σ_k in Equation 4, it is strongly suggested that for the tiny ZnO particles a cavitation mechanism dominates. Also in Table I, the elongation at break is seen to increase significantly as the molecular weight increases from 6000 to 17 250 kDa, and continues to increase when the molecular weight is increased to 120 000 kDa. At the same time, the tensile strength remains constant at around 40 p.s.i. Since the highest molecular-weight resin has the largest elongation at break ε_b, the failure process which leads to wear loss should not start in the bulk of the rubber phase, but rather should originate near the rigid particles, the stressed zones where cavitation can take place.

TABLE I Mechanical properties of neat resins

M_w of pre-cured PDMS	Elongation at break, ε_b (%)	Tensile strength, σ_b (p.s.i.)	Young's modulus, E_1 (p.s.i.)
6000	40	40	120
17 250	310	50	55
120 000	410	40	30

Since the highly stressed regions surrounding the rigid particles are important in the wear of filled rubbers, we can further define a 'damage zone' near the particles as where the tri-axial tension, τ, exceeds a material parameter $\hat{\sigma}_b$. The material parameter $\hat{\sigma}_b$ is the mechanical strength of the rubber material in the highly stressed region, the stressed zones, and should be dependent on the critical stresses of debonding and cavitation which are influenced by the degree of reinforcement, thermal stability, etc. By prescribing a value for $\hat{\sigma}_b$, the total volume of the damage zones, V_{dz}, in the composite can be estimated. It is interesting to examine how the volume of the damage zones correlates with the observed wear rates. To estimate the damage zone volume, the stress fields extending from the close particles must be considered. The angular dependence of the tri-axial tension τ

$$\frac{\tau}{T_\infty} = 1 + \frac{(1 + 3\cos 2\theta)}{4}\left(5\frac{a_0^3}{r^3}\right) \qquad (5)$$

shows that τ is maximal when $\theta = 0, \pi$, i.e., in the directions parallel to the externally applied stress. As $|\theta|$ increases from 0, τ decreases and the second term in Equation 5 of the induced component eventually becomes negative when $|\theta|$ reaches 54.7°. This means that relative to a single particle in a rubber matrix the material in the regions near the equator, $\pi/2 - 35.3° < |\theta| < \pi/2 + 35.3°$, is under a compressive influence from the filler. Conversely, when considering the stress fields in any small area close to a rigid particle, of interest in a filled rubber, if any of the other filler particles lie within the compressive range, $\pi/2 - 35.3° < |\theta| < \pi/2 + 35.5°$, relative to that particle, there will be no contribution of dilatational influences from these particles and therefore these particles can be ignored when calculating the tri-axial tension. For simplicity, however, the tri-axial tension at the poles, where τ is the greatest, of a one dimensional lattice of particles is first calculated. Expressed as a sum of the stress fields of all the rigid particles, τ can be expressed as

$$\begin{aligned}\frac{\tau}{T_\infty} &= 1 + 5a_0^3\left[\frac{1}{(s - \tilde{r})^3} + \frac{1}{(s + \tilde{r})^3}\right] \\ &\quad + 5a_0^3\left[\frac{1}{(3s - \tilde{r})^3} + \frac{1}{(3s + \tilde{r})^3}\right] + \cdots \\ &= 1 + 10\left(\frac{a_0}{s}\right)^3 \sum_{n=1}^{\infty} \frac{1 + 3\left(\frac{\tilde{r}}{ns}\right)^2}{n^3\left[1 - \left(\frac{\tilde{r}}{ns}\right)^2\right]^3} \qquad (6)\end{aligned}$$

where s is the half spacing between the particles, $\tilde{r} \equiv r - s$, and $n = 1$ represents the first nearest neighbours and so forth. As mentioned before, the induced stresses decay very rapidly with r. For low filler concentration, 10 wt % for example, only around 2% of the applied stress T_∞ is extended from the nearest particles of the

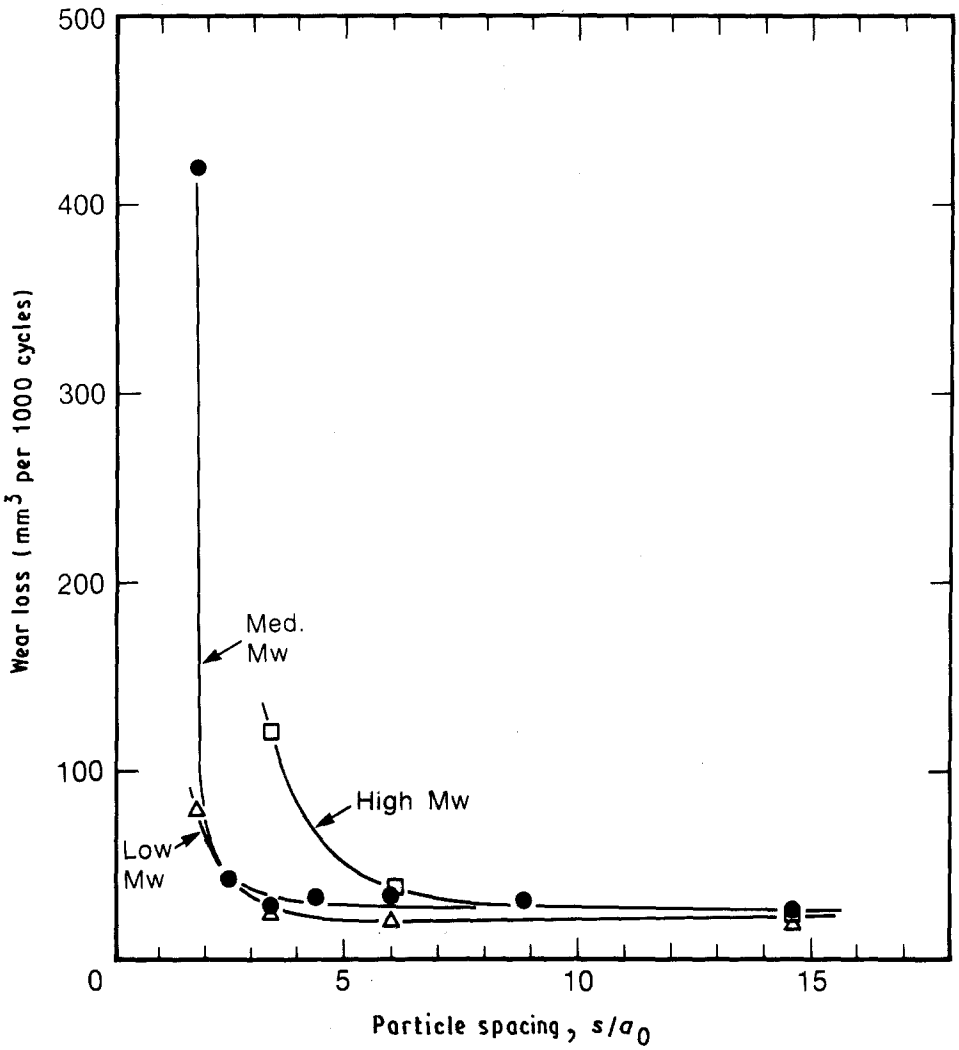

Figure 10 Normalized wear rate against filler concentration for the three molecular-weight matrices filled with zinc oxide (ZnO in PDMS). M_w □, high, 120 000; ●, medium, 17 250; △, low, 6000 kDa.

dilatational range. Even for high filler concentration of 80 wt %, although the tension from the nearest particles is quite high (approximately 115% of T_∞), that contribution decreases rather quickly to 6% of T_∞ for the second nearest particle and to less than 3% for the third. When $\theta \neq 0, \pi$, the stress starts as a small fraction of T_∞, approximately 6% for $n = 1$, and decays even faster. Therefore in a three-dimensional case, the tension at the poles of each particle can be regarded approximately as the sum of the stresses from particles lying on the plane $\theta = 0$ superimposed by the relatively small compressional stresses from particles at $\theta = \pi/2$.

However, for the purpose of illustration, the damage zone volume V_{dz} was calculated using the tri-axial tension from Equation 6, and the angular dependence of τ was ignored assuming the damage zones were isotropically surrounding each particle. The latter assumption is clearly not realistic, but since we are more interested in how V_{dz} varies with filler concentration rather than the absolute values, the results should still represent what actually happens and provide us with insight to the problem. Fig. 11 shows the calculated tri-axial tension τ for the case of ZnO (density, $\rho = 5.6$) from 10 to 80 wt %, and Fig. 12 shows the corresponding values of V_{dz} using a prescribed material parameter, $\hat{\sigma}_b$, normalized to the total rubber volume, V_0. Compared to the wear data of ZnO, the similarity is striking. The volume of the damage zones where the microcavitational processes are most likely to take place correlates very well with the observed wear behaviours. It therefore indicates that the observed filler effects are due to the stress concentrations from these rigid particles, and can be understood from this simple approach. The portion of the curve of V_{dz}/V_0 in the low filler concentration regime appears to be lower compared to the shape of the wear rate. This, however, is believed to be due to the effect of the sharp asperities on the abrasive counterpart, that tends to smooth the stress concentration effect from the filler particles especially when the latter is relatively small. The calculated result in Fig. 12 assumes the material parameter $\hat{\sigma}_b = 5.0\ T_\infty$, but a range of $\hat{\sigma}_b$ values have been calculated. It is found that the choice of $\hat{\sigma}_b$ value can change the location of the critical filler fraction and the slope of the wear rate in the second wear regime, but the characteristics of the curve remain unchanged. Most importantly, from this result we can assert that the critical filler fraction, v_c, represents the onset of effective stress overlapping that in turn yields a dramatic increase in the damage zone volumes.

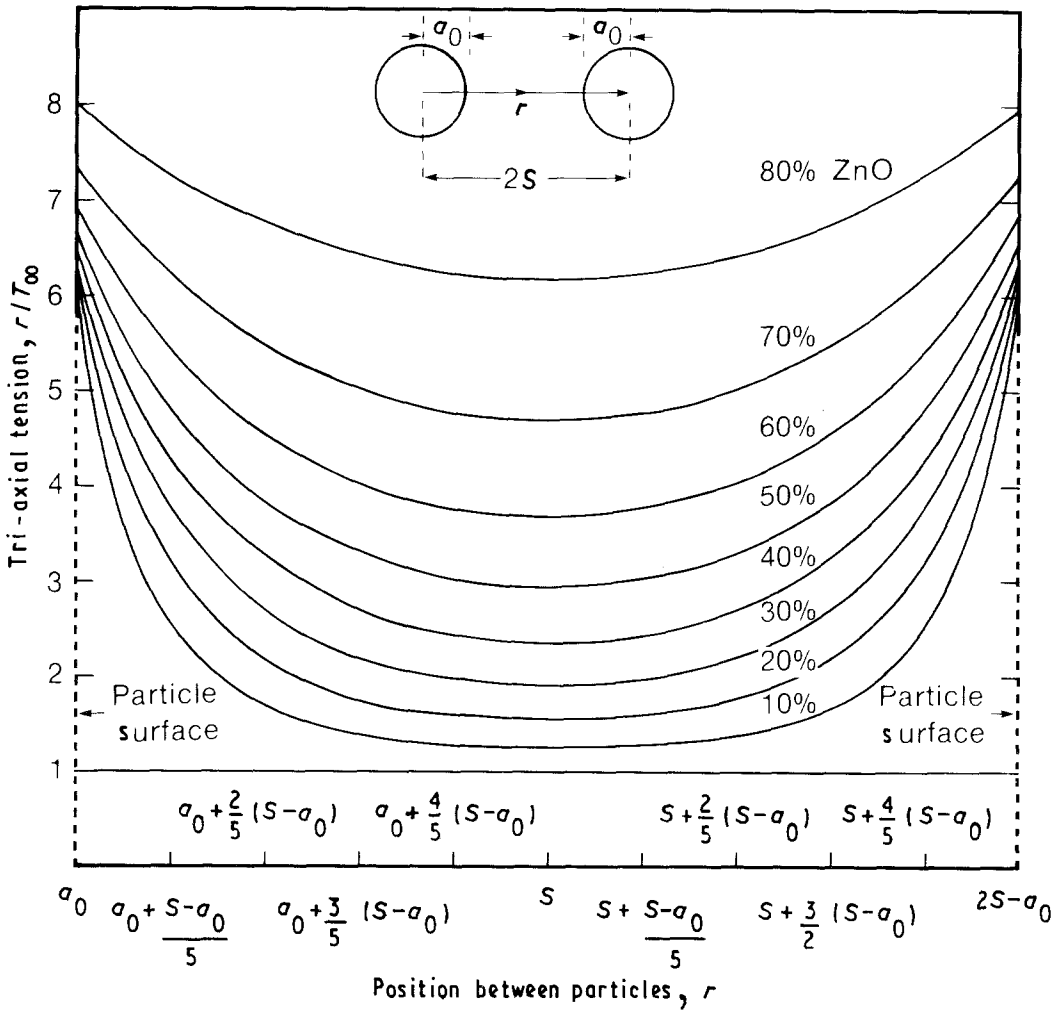

Figure 11 Calculated tri-axial tension, τ, between two nearest particles in the one-dimensional filler particle lattice.

4. Discussion

The results presented above strongly indicate that the highly stressed rubber layers associated with the rigid filler particles are sources of weakness in the filled elastomers during abrasive wear. The highly stressed regions harbour the microscopic damage processes of cavitation and/or debonding, that later develop into cracks, leading to material removal. As clearly demonstrated, the volume of the damage zones is a convenient and useful means to quantify the degree of this weakness. From the experimental data obtained, we speculate that cavitation near the filler particles probably dominates the cases where very tiny filler particles are used, while for large filler particles debonding prevails. The material strength, $\hat{\sigma}_b$, used here to define the damage zone, although artificial, is a natural parameter that carries the most important information on the fundamental filler reinforcement and wear resistance. If we can measure it independently and understand how it behaves, we will undoubtedly have a much better understanding of the filler's role in composite reinforcement, and therefore have a better understanding of how to create materials for predictable wear.

The stress concentration at the edge, $\theta = 0, \pi$, of the rigid particles has been shown to increase steadily [18] as the particle aspect ratio increases when the long axis is parallel to the external stress T_∞. This result is valid for both the short fibres and platelets. Our SEM pictures of the cross-section surfaces of the mica and the short glass-fibre composites reveal that these particles, when embedded in the elastomer, are actually aligned in the direction normal to the sample thickness, the same direction as the abrasion action. Since the critical filler fraction, v_c, is the onset of the effective stress-field overlapping, a lower critical filler fraction should be expected for a higher aspect ratio filler.

The rigid filler particles, however, are not always detrimental in terms of abrasion resistance. As shown in Fig. 9, the filled low molecular-weight PDMS actually shows improved wear resistance when compared to the unfilled resin in the first wear regime. This effect is believed to be due to the effective filler reinforcement. Since the first wear regime is controlled by the intrinsic wear mechanisms of the neat resin where the improved mechanical properties can enhance the wear resistance, mechanical reinforcement by the filler particles can compensate for damage initiation in the stressed zone and hence show a lower wear rate in the composites.

There are several limitations on when this damage-zone concept can apply. Since the damage-zone concept is based on the micro-cavitational mechanisms

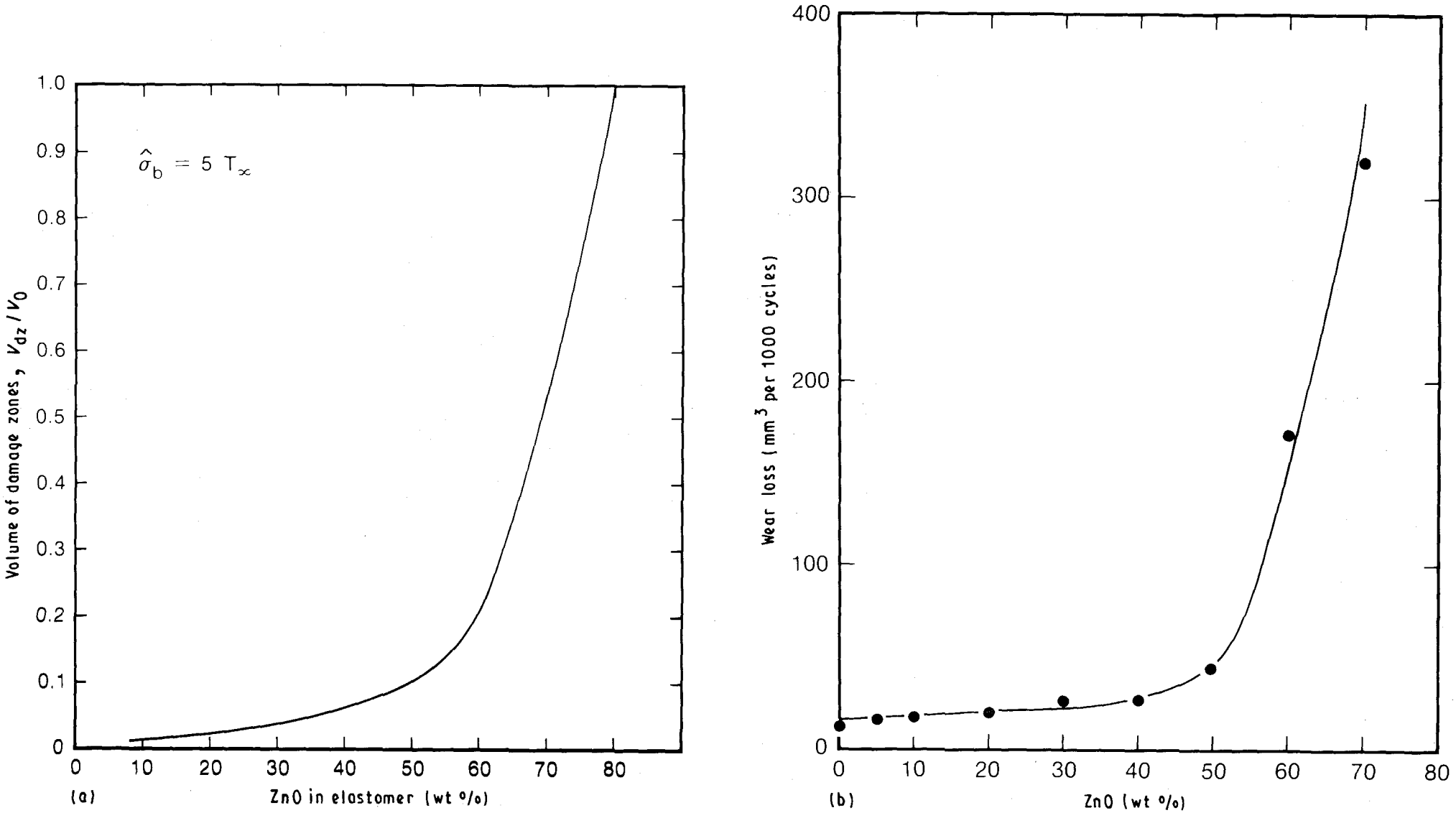

Figure 12 (a) Calculated normalized damage zone volume V_{dz}/V_0 against zinc oxide particle concentration; (b) wear rate against weight fraction of zinc oxide in a filled silicone elastomer.

that eventually lead to failure, if fillers cannot trigger these processes, good correlation between the damage-zone volume and the wear rate may be absent. Carbon blacks, noted for their effects on improving the wear of some rubbers, are not included in this study because they tend significantly to change the cure characteristics of the silicone rubbers. It is conceivable, however, that when the particles become very small, ~ 5 nm for instance, either debonding or cavitation would be very difficult to initiate. Since carbon blacks reinforce the rubber significantly, this may explain why the wear is improved in these cases. Another exception also includes the chemical effect from the individual filler species where free radicals strongly react with the fillers [10–12]. The damage zone concept can still apply in these cases, but when the free radical interaction becomes dominant, the chemical aspects of wear must also be considered.

5. Conclusions

1. Rigid filler particles normally increase the abrasive wear loss of the filled silicone elastomers. There exists a critical filler fraction, v_c, which divides two regimes of wear that apparently operate by different mechanisms.

2. The first regime, where the filler concentration is low, is dominated by the properties of the neat resin. The increase of wear rate due to the filler is gradual here. In the cases of effective filler reinforcement, a reduction of wear rate can occur.

3. The second regime is dominated by the filler's detrimental effects where the wear rate increases very rapidly with filler concentration. The stress concentration introduced by the rigid particles effectively creates a 'damage zone' surrounding the particles, a location where micro-cavitation and debonding takes place. Cavitation appears to dominate in the composites of very small filler particles, while debonding dominates when larger particles are involved.

4. Higher particle aspect ratio and/or poor adhesion at the rubber–particle interface leads to a lower critical filler fraction of the filled elastomer.

5. The calculated volume of the damage zones, V_{dz}/V_0, correlates with the wear rate. It indicates that the critical filler fraction, v_c, is the onset of the stress overlapping between particles.

Acknowledgements

We would like to thank Dr J. Hedrick for providing the catalyst system for some of the silicone rubbers, and Dr C. K. Lee for stimulating discussion on micromechanics. We would also like to extend our gratitude to Dr C. Ortiz for letting us test her sputtered thin film for peel tests, and to J. Duran for his help in SEM. The helpful discussion with Professor A. N. Gent of the University of Akron is also acknowledged.

References

1. A. SCHALLAMACH, *Wear* **1** (1958) 384.
2. J. K. LANCASTER, *J. Phys. D* **1** (1968) 549.
3. *Idem, Wear* **14** (1969) 223.
4. S. B. RATNER and N. V. MELNIKOVA, *Kauchuk i Rezina* **17** (1958) 14.
5. *Idem, Rubber Chem. Tech.* **32** (1959) 1199.
6. S. B. RATNER, I. I. FARBEROVA, O. V. RADYUKEVICH and E. B. LURE, *Sov. Plast.* **7** (1964) 37.
7. E. SOUTHERN and A. G. THOMAS, *Plast. Rubber Mater. Applic.* **3** (1978) 133.
8. D. H. CHAMP, E. SOUTHERN and A. G. THOMAS, in "Advances in Polymer Friction and Wear", edited by L.-H. Lee (Plenum, New York, London, 1974) p. 133.
9. A. SCHALLAMACH, *J. Appl. Polym. Sci.* **12** (1968) 281.
10. A. N. GENT and C. T. R. PULFORD, *ibid.* **28** (1983) 943.
11. A. N. GENT and B. PARK, *J. Mater. Sci.* **19** (1984) 1947.
12. A. N. GENT and W. R. RODGERS, *J. Polym. Sci., Polym. Chem. Ed.* **23** (1985) 829.
13. M. K. KAR and S. BAHADUR, *Wear* **30** (1974) 337.
14. K. TANAKA and S. KAWAKAMI, *ibid.* **79** (1982) 221.
15. L. J. BROUTMAN and R. H. KROCK, "Modern Composite Materials", (Addison-Wesley, Reading, MA, 1967) ch. 2.
16. J. N. GOODIER, *Trans. ASME* **55** (1933) 7.
17. E. O. HALL, *Proc. Phys. Soc. (Lond.)* **64B** (1951) 747.
18. N. J. PETCH, *J. Iron Steel Inst., Lond.* **174** (1953) 25.

Received 27 July 1990
and accepted 6 February 1991